

LASERS

PACS numbers: 42.55.Px; 42.60.Lh; 85.60.Jb
DOI: 10.1070/QE2011v041n08ABEH014652

Broadband superluminescent diodes and semiconductor optical amplifiers for the spectral range 750 – 800 nm

S.N. Il'chenko, Yu.O. Kostin, I.A. Kukushkin, M.A. Ladugin,
P.I. Lapin, A.A. Lobintsov, A.A. Marmalyuk, S.D. Yakubovich

***Abstract*. We have studied superluminescent diodes (SLDs) and semiconductor optical amplifiers (SOAs) based on an $(Al_xGa_{1-x})As/GaAs$ single quantum well structure with an Al content $x \sim 0.1$ in a 10-nm-thick active layer. Depending on the length of the active channel, the single-mode fibre coupled cw output power of the SLDs is 1 to 30 mW at a spectral width of about 50 nm. The width of the optical gain band in the active channel exceeds 40 nm. Preliminary operating life tests have demonstrated that the devices are sufficiently reliable.**

Keywords: *superluminescent diode, semiconductor optical amplifier, quantum well heterostructure.*

1. Introduction

There are a number of SLD-based high-efficiency near-IR (800 – 1100 nm) light sources. Broadband SLDs with emission bandwidths above 50 nm are of particular interest for many practical applications [1 – 4]. Such SLDs are commonly fabricated using semiconductor heterostructures with quantum well active layers and operate at considerably higher nonequilibrium carrier concentrations in comparison with analogous laser diodes. This enables intrinsic spontaneous emission amplification corresponding to quantum transitions not only from the main band but also from excited subbands of the energy spectrum. One distinctive feature of SLDs based on quantum size structures is that the shape of their (typically double-humped) emission spectrum strongly depends on the configuration of the active channel and operation conditions.

There are also sufficiently powerful SLD sources (Superlum, Exalos, InPhenix, Qphotonics and others) operating at the long-wavelength edge of the visible spectrum (750 – 800 nm), but their spectral width does not exceed 22 nm. Such SLDs are based on heterostructures with bulk or quantum well active layers from (GaAl)As or (InGa)AsP. In the case of quantum well active layers, the superluminescence is only contributed by quantum transitions from the ground state. As shown by Miyake et al. [5], InP quantum dots in (GaIn)P layers lattice-matched to GaAs have a broad photoluminescence band ($\Delta\lambda \sim 50$ nm) in the spectral range in question, but to the best of our knowledge no injection lasers or SLDs based on such structures have been demonstrated.

Earlier, we attempted to develop broadband quantum well SLDs for this spectral range. At injection current densities of 7 – 8 kA cm^{-2}, the output spectral width of prototype devices was above 40 nm, but their lifetime was within 100 h. At lower current densities, their operation was reliable enough, but the full width at half maximum (FWHM) of their bell-shaped emission spectrum was 15 – 20 nm.

In this paper, we describe efficient, sufficiently reliable SLDs with a centre wavelength near 780 nm and emission bandwidth of about 50 nm that have been fabricated through the use of technological advancements reported previously by Lobintsov et al. [6] and optimisation of the ionic cleaning of the end facets of SLDs before anti-reflection coating deposition.

2. Experimental samples and results

The SLDs were based on an $(Al_xGa_{1-x})As/GaAs$ single quantum well (SQW) structure with an Al content $x \sim 0.1$ in a 10-nm-thick active layer. The energy band diagram of the SQW structure is presented in Fig. 1. We used a widespread SLD design with a straight ridge waveguide inclined at 7° to the normal to the end facets of the crystal. To further suppress optical feedback, an Al_2O_3/ZrO_2 two-layer anti-reflection coating was deposited onto the end facets. Before the coating process, the cleaved surface was

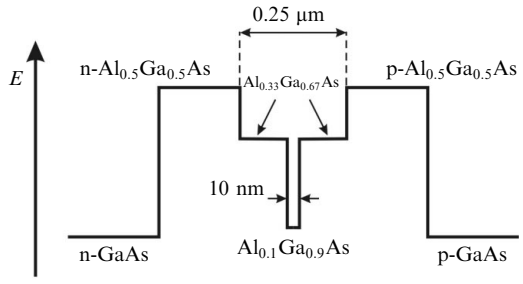

Figure 1. Energy band diagram of a (GaAl)As/GaAs single quantum well structure.

S.N. Il'chenko, Yu.O. Kostin, I.A. Kukushkin, M.A. Ladugin, P.I. Lapin, A.A. Lobintsov, A.A. Marmalyuk, S.D. Yakubovich Superlum Diodes Ltd., P.O. Box 70, 117454 Moscow, Russia;
e-mail: i_a_kukushkin@mail.ru

Received 6 May 2011
Kvantovaya Elektronika **41** (8) 677 – 680 (2011)
Translated by O.M. Tsarev

cleaned by low-energy (about 50 eV) argon ions to remove contamination and oxides. To this end, we used a Kaufman type ion source, which produced an argon ion beam in the vacuum chamber. The cleaning of the end facets and subsequent anti-reflection coating deposition were performed in a single vacuum cycle. When the layers were grown through electron beam sputtering, the coating was exposed to argon ions with an average energy of 100 eV. The thickness of the active waveguide was 0.25 μm, its width was 4 μm, and its length was varied from 700 to 1600 μm in 100-μm steps. The measurements were made using cw injection, and the pump current and temperature were stabilised by a PILOT-4 controller.

Figure 2a illustrates the effect of injection current on the emission spectrum of the SLDs. The spectrum comprises two, well-resolved peaks near 760 and 790 nm, due to the quantum size effect. Typical dependences of the free-space output power, P_{FS}, on injection current at different lengths of the active channel are presented in Fig. 2b. The optimal injection current of SLDs with such a shape of their emission spectrum is that at which the peaks are equal in intensity and the FWHM of the spectrum reaches a maximum, which corresponds to the minimum coherence length. In Fig. 2b, the optimal injection currents at different lengths of the active channel are marked by filled circles. (At an active channel length of 1600 μm, we failed to equalise the intensities of the peaks at acceptable injection currents.)

The main spectral and power parameters of the SLDs under optimal operation conditions are listed in Table 1.

Figure 3 shows the central peak of the intensity autocorrelation function (ACF) for the SLDs under consideration. The secondary peaks of the ACF are hardly discernible from the background level because the residual Fabry–Perot modulation depth is very small.

We performed preliminary SLD life tests under typical operation conditions, at a stabilised current and a temperature of 25 °C. The curves in Fig. 4 illustrate the degradation of the SLDs tested. Linearly extrapolating the curves, we were able to estimate the average lifetime of the SLDs: 4000–7000 h for the SLDs with a double-humped emission spectrum and 10 000 h for the SLDs with a bell-shaped spectrum.

The SLDs under consideration have considerable potential for use in BroadLighter broadband combination light sources, which take advantage of radiation from several SLDs with partially overlapping spectra and employ broadband fibre couplers [7]. Figure 5 shows the output spectrum of a prototype two-channel combination source that utilises the SLD examined in this study as a short-wavelength source. With a spectral width of 105 nm and a coherence length of about 6.0 μm, this light source (tentative name: BroadLighter-D-810) is the shortest wavelength device in the series in question.

Comparison of the superluminescence spectra of SLDs

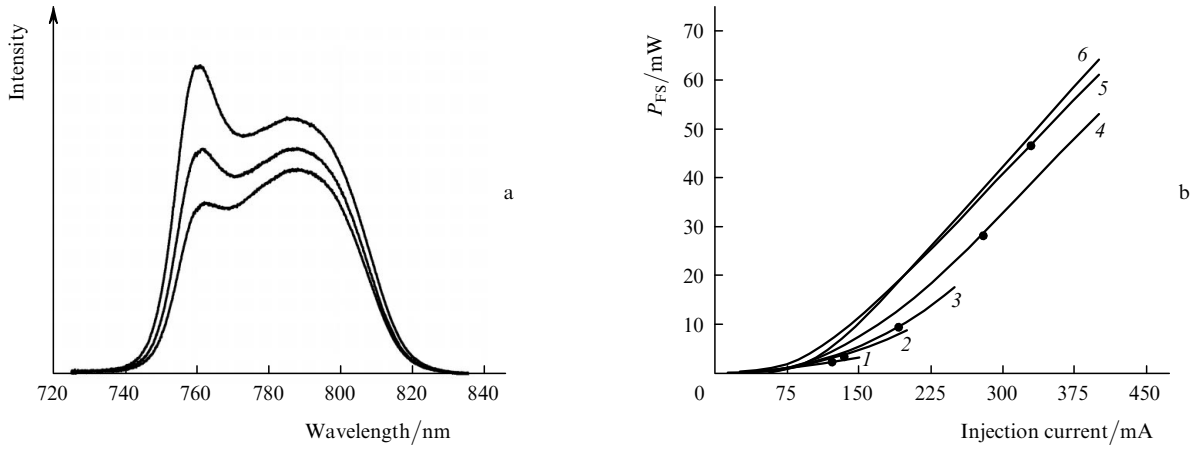

Figure 2. (a) Effect of injection current on the output emission spectrum of the SLDs. (b) Light–current characteristics of the SLDs with an active channel length of (*1*) 700, (*2*) 800, (*3*) 1000, (*4*) 1200, (*5*) 1300 and (*6*) 1600 μm.

Table 1. Parameters of the SLDs at different lengths of the active channel under optimal operation conditions (L_a = 700 – 1300 μm) and for a bell-shaped emission spectrum (L_a = 1600 μm).

L_a/μm	I/mA	J/kA cm^{-2}	P_{FS}/mW	P_{SM}/mW	λ_m/nm	$\Delta\lambda$/nm	δS (%)	L_c/μm
700	115	4.1	3.10	1.0	779.5	54.4	12	11.2
800	135	4.2	4.15	1.7	781.3	51.9	19	11.8
900	170	4.7	6.05	3.0	782.5	50.6	17.5	12.1
1000	190	4.8	10.2	5.4	782.7	49.5	19	12.4
1100	205	4.7	16.8	9.0	782.4	48.8	21	12.5
1200	265	5.6	28.1	17.6	782.1	47.5	21.5	12.9
1300	344	6.3	55.6	30.4	781.7	47.3	25	12.9
1600	320	5.0	57.6	32.2	790.8	24	–	26.1

Note: L_a is the length of the active channel, I is the injection current, J is the injection current density, P_{FS} is the free-space output power, P_{SM} is the single-mode fibre coupled output power (we used Corning Pure Mode 720 fibre, optimal for the spectral range of interest, with a cylindrical microlens at its input end), λ_m is the median wavelength, $\Delta\lambda$ is the FWHM of the emission spectrum, δS is the depth of the minimum in Fig. 2a, and L_c is the coherence length evaluated as $L_c = \lambda^2/\Delta\lambda$.

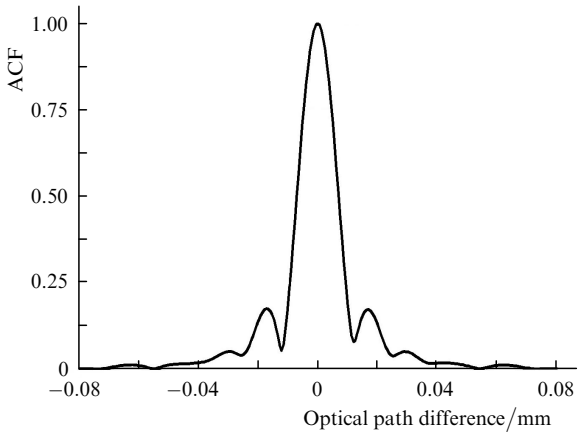

Figure 3. Central peak of the intensity autocorrelation function for the SLDs ($L_a = 1000$ μm, $I = 225$ mA).

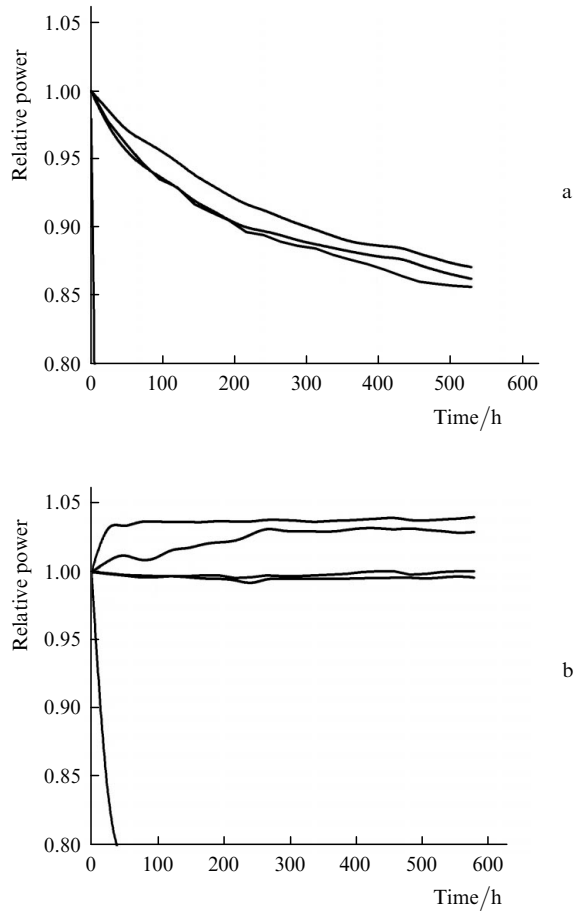

Figure 4. Preliminary SLD life test results at an active channel length of (a) 1000 and (b) 1600 μm.

at different active channel lengths and identical injection current densities allows one to evaluate the optical gain per unit length spectrum and the net small-signal gain G as a function of sample length [8]. Figure 6 presents such calculation results for $L_a = 1100$ μm. In particular, at a current density $J = 3000$ kA cm^{-2} the gain band width is about 40 nm at a level of 0.5 and about 50 nm at a level of 0.1. We plan to fabricate SOA modules based on the active elements studied here, with input/output single-mode fibre pigtails.

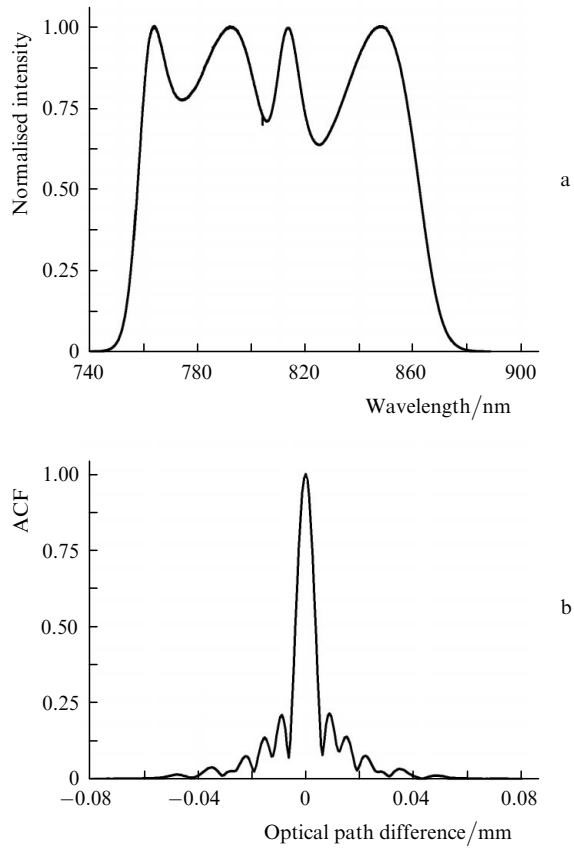

Figure 5. (a) Output spectrum of a new BroadLighter combination light source that utilises one of the SLDs examined in this study; (b) central peak in its ACF.

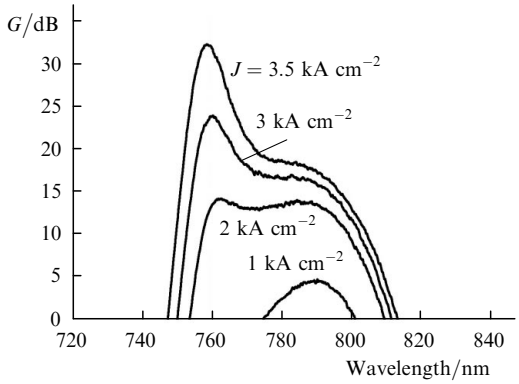

Figure 6. Small-signal gain spectra at different current densities.

3. Conclusions

We have demonstrated the first high-efficiency, sufficiently reliable broadband SLDs with a centre wavelength of 780 nm. Varying the length of the active channel, we can obtain single-mode fibre coupled cw output powers in the range 1 to 30 mW at an FWHM of the spectrum near 50 nm. The devices can be used as active elements of SLD and SOA modules.

Acknowledgements. We acknowledge stimulating discussions with A.T. Semenov. This work was supported in part by the Federal Agency for Education (Project No. 2.1.1.12404).

References

1. Batovrin V.K., Garmash N.A., Gelikonov V.M., Gelikonov G.V., Lyubarskii A.V., Plyavenek A.G., Safin S.A., Semenov A.T., Shidlovskii V.R., Shramenko M.V., Yakubovich S.D. *Kvantovaya Elektron*., **23** (2), 113 (1996) [*Quantum Electron*., **26** (2), 109 (1996)].
2. Mamedov D.S., Prokhorov V.V., Yakubovich S.D. *Kvantovaya Elektron*., **33** (6), 471 (2003) [*Quantum Electron*., **33** (6), 471 (2003)].
3. Lapin P.I., Mamedov D.S., Marmalyuk A.A., Padalitsa A.A., Yakubovich S.D. *Kvantovaya Elektron*., **36** (4), 315 (2006) [*Quantum Electron*., **36** (4), 315 (2006)].
4. Kostin Yu.O., Lapin P.I., Prokhorov V.V., Shidlovsky V.R., Yakubovich S.D. *Proc. SPIE–Int. Soc. Opt. Eng*., **7139**, 713905-1 (2008).
5. Miyake S., Lee W.S., Ujihara T., and Takeda Y. *Proc. Indium Phosphide and Related Materials Conf.* (Princeton, 2006) p. 208.
6. Lobintsov A.A., Uspenskii M.B., Shishkin V.A., Shramenko M.V., Yakubovich S.D. *Kvantovaya Elektron*., **40** (4), 305 (2010) [*Quantum Electron*., **40** (4), 305 (2010)].
7. Adler D.S., Ko, T.H., Konorev A.K., Mamedov D.S., Prokhorov V.V., Fujimoto J.J., Yakubovich S.D. *Kvantovaya Elektron*., **34** (10), 915 (2004) [*Quantum Electron*., **34** (10), 915 (2004)].
8. Goldobin I.S., Semenov A.T., Tabunov V.P., Yakubovich S.D. *Kvantovaya Elektron*., **9** (6), 1264 (1982) [*Sov. J. Quantum Electron*., **12** (6), 800 (1982)].